International Journal of Advanced Engineering and Technology Research
ISSN: 3106-8677 (Print), ISSN: 3106-8685 (Online) | Vol. 1, No. 1, 2026

Observation of Topological Corner States in a Kagome Circuit

Xiaochan Wang

School of Guangdong University of Technology, Guangzhou 510000, China

Abstract: Higher-order topological insulators enable energy localization at boundaries such as corners. Circuit platforms offer tunable components and flexible lattice design for simulating such topological states. Here, we implement a breathing Kagome lattice in an electric circuit network, where intra-cell and inter-cell couplings are independently controlled by capacitance values. Impedance spectroscopy and voltage mapping directly reveal topological corner states localized at two adjacent corners, with energies inside the bulk gap. These states emerge only under specific coupling conditions and remain robust against circuit parameter disorder. Our work demonstrates the feasibility of studying higher-order topology in Kagome lattices using circuit networks and offers a new route for exploring tunable topological corner states and their potential applications.

Keywords: Topological corner states; Kagome lattice; Circuit network; Higher-order topology.

1. Introduction

The discovery of topological insulators has fundamentally reshaped modern condensed matter physics, establishing that materials can be classified by topological invariants beyond the conventional paradigm of symmetry breaking [1,2]. A hallmark of these systems is the bulk–boundary correspondence, wherein a nontrivial bulk topology guarantees the emergence of gapless boundary states. More recently, this concept has been generalized to higher-order topological insulators (HOTIs), which host boundary states at even lower dimensions [3,4]. In a d-dimensional nth-order topological insulator, topologically protected modes reside on $(d-n)$-dimensional boundaries. In two dimensions, for instance, second-order topological insulators support zero-dimensional corner states—modes tightly localized at the corners of a finite sample. Such corner states have attracted growing interest owing to their potential for robust waveguiding, quantum information processing, and high-sensitivity sensing [5,6].

The Kagome lattice, a two-dimensional network formed by corner-sharing triangles, has attracted considerable attention as a platform for topological physics owing to its distinctive band structure, which features flat bands, Dirac cones, and quadratic band touching points [7,8]. In particular, the breathing Kagome lattice, characterized by alternating intra-cell and inter-cell hopping amplitudes, has been theoretically predicted to support higher-order topological phases with corner-localized states [9,10]. Experimental demonstrations of such corner states have since been reported in photonic lattices [11], phononic crystals [12], and mechanical metamaterials [13]. Despite these advances, the limited tunability and fabrication complexity inherent to these platforms have motivated the exploration of more flexible and reconfigurable alternatives. Electrical circuit networks have recently emerged as a versatile platform for simulating topological band structures [14,15]. By mapping tight-binding Hamiltonians onto circuit Laplacians, topological phases can be realized using elementary components such as capacitors, inductors, and operational amplifiers. Key advantages of circuit implementations include the ability to engineer arbitrary lattice geometries, independently control coupling strengths via component values, and directly probe topological states through impedance measurements [16,17]. These features render circuits particularly well suited for investigating higher-order topology, where precise control over intra-cell and inter-cell couplings is essential for accessing the topological phase.

In this work, we experimentally implement a breathing Kagome lattice using an electric circuit network and observe the manifestation of topological corner states. By adjusting capacitance values, we achieve independent control over intra-cell and inter-cell couplings, enabling the engineering of a higher-order topological phase characterized by a quantized quadrupole moment. Through impedance measurements and voltage mapping, we directly image corner-localized modes whose frequencies lie within the bulk band gap. These corner states emerge exclusively in the topological configuration and remain robust against moderate disorder in circuit parameters. Our findings establish circuit networks as a versatile platform for exploring higher-order topology in frustrated lattices and open new avenues for reconfigurable topological devices.Results and Discussion.

2. Results and Discussion

2.1. Kagome Circuit model

Figure 1 shows a schematic illustration of an infinite breathing kagome lattice constructed from LC circuits. The circuit network consists of periodically arranged nodes, each corresponding to a lattice site of the kagome geometry. Nodes are connected through capacitors, with intra-cell coupling capacitors denoted as C_A (purple connections in Fig. 1) and inter-cell coupling capacitors denoted as C_B (yellow connections in Fig. 1). Each node is grounded via an inductor L, forming a parallel resonant circuit. This design allows the circuit dynamics to be precisely described by a tight-binding model, where the capacitance values directly correspond to hopping strengths and the inductors provide the on-site grounding terms. By adjusting the relative values of the capacitances C_A and C_B, we can independently control the intra-cell and inter-cell coupling strengths, thereby realizing a transition from a topologically trivial phase to a topologically nontrivial phase. To quantitatively characterize this process,

we calculated the bulk band structure of the system for different parameter sets, as shown in Figure 2. The band calculations are performed along high-symmetry lines in the Brillouin zone, with the horizontal axis k representing the momentum space path and the vertical axis representing the eigenvalues.

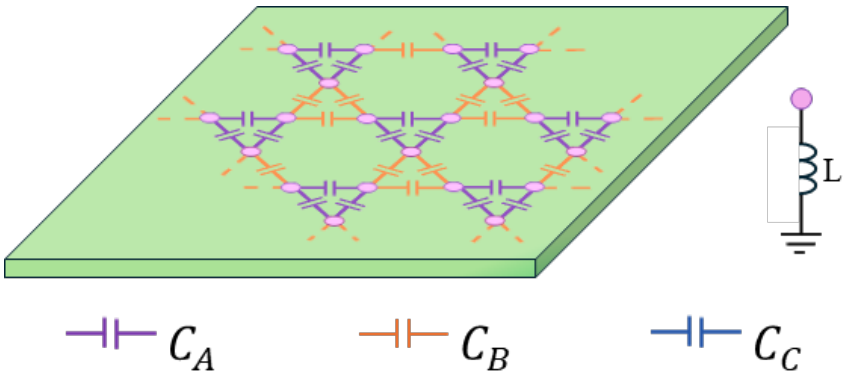

Fig. 1 Illustration of the infinite Kagome LC circuit.

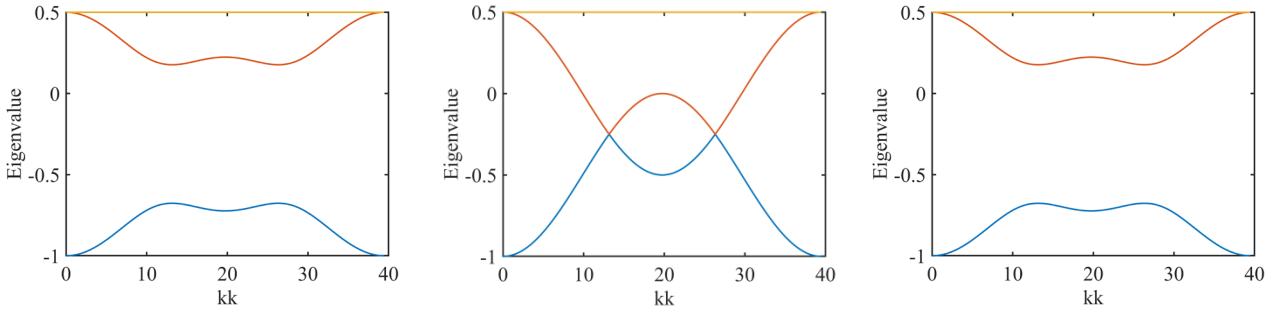

Fig. 2 (a), (b), (c) Bulk dispersions of the Kagome LC circuit with $C_A = 2.2nF, C_B = 8nF; C_A = 3nF, C_B = 3nF; C_A = 8nF, C_B = 2.2nF;$ they both share parameters $L = 1\mu H$.

Figure 2(a) displays the band structure for $C_A = 2.2nF, C_B = 8nF, L = 1\mu H$. In this case, a finite band gap opens in the bulk spectrum, indicating that the system is in a topologically nontrivial phase. Figure 2(b) corresponds to the case $C_A = 3nF, C_B = 3nF$,, where the bands close, forming a Dirac cone and marking a topological phase transition. Figure 2(c) shows the band structure for $C_A = 8nF, C_B = 2.2nF$, where the bulk gap reopens, but the system enters a topologically trivial phase. The insets in each subfigure illustrate the corresponding capacitance configurations.

From this band evolution, we can clearly summarize the topological phase transition rule for the breathing kagome lattice:When $C_A < C_B$, the system is in a topologically nontrivial phase, where corner-localized states are expected to appear in finite-sized samples. When $C_A > C_B$, the system is in a topologically trivial phase with no corner states. When $C_A = C_B$, the band gap closes, corresponding to a topological phase transition point. In the following experiments, we will employ a finite-sized triangular circuit network with well-defined corners to facilitate the observation of corner-localized states.

2.2. Hamiltonian

In the circuit, the capacitors C_A and C_B corresponds to the tight-binding parameters. Each node is grounded through an inductor L, forming a parallel resonant circuit. Under AC excitation, the dynamics of the circuit are governed collectively by Kirchhoffs laws and Ohms law. Considering harmonic voltage excitation at frequency ω, the nodal voltage vector is denoted as $V = [V_1, V_2, V_3]^T$, and the current injection vector as $I = [I_1, I_2, I_3]^T$. According to Kirchhoffs current law, the net current at each node is zero, leading to:

$$I(\omega) = J(\omega)V(\omega), \tag{1}$$

where J(ω) is the circuit admittance matrix, also referred to as the circuit Laplace operator. For a linear passive network composed of capacitors and inductors, J(ω) can be expressed as:

$$J(\omega) = i\omega C + \frac{1}{i\omega L}E, \tag{2}$$

here, C is the capacitive coupling matrix, and E is the identity matrix. In our bilayer Kagome circuit, the off-diagonal part of C directly corresponds to the tight-binding Hamiltonian H, while the diagonal contribution arises from the grounding inductors via the term $\frac{1}{i\omega L}E$. By introducing the variable substitution $\lambda = \omega^2 LC$, the circuit equation can be recast as an eigenvalue problem:

$$HV = \lambda V, \tag{3}$$

where H is precisely the effective tight-binding Hamiltonian to be derived. The Hamiltonian in momentum space is represented by a 3×3 matrix:

$$H = \begin{pmatrix} 0 & Q_1 & Q_2 \\ Q_1^* & 0 & Q_3 \\ Q_2^* & Q_3^* & 0 \end{pmatrix} \tag{4}$$

where the matrix elements defined by:

$$Q_1 = C_A + C_B e^{-i\left(\frac{k_x}{2} + \frac{\sqrt{3}k_y}{2}\right)}, Q_2 = C_A + C_B e^{-ik_x}, \ Q_3 = C_A + C_B e^{-i\left(\frac{k_x}{2} - \frac{\sqrt{3}k_y}{2}\right)}, \tag{5}$$

which $k = (k_x, k_y)$ is the wave vector within the two-dimensional Brillouin zone. The block structure of this Hamiltonian is evident.

2.3. Topological Corner States

To demonstrate the existence of corner states in the Kagome circuit model, we constructed a finite-sized circuit network comprising 30 nodes (15 unit cells). The network

geometry was designed as a triangle, a configuration that facilitates the observation of corner-localized states. By calculating the admittance spectrum and eigenfrequency spectrum of the circuit, we identified localized states at specific frequencies. When the intra-cell coupling capacitance $C_A = 2.2nF$, inter-cell coupling capacitance $C_B = 8nF$, and grounding inductance $L = 1\mu H$, the system is in a topologically nontrivial phase with $C_A < C_B$. Under these parameters, theory predicts the existence of three degenerate topological corner states inside the bulk gap. Our calculations show that these corner states appear at frequency $f =$ 352.3 kHz, precisely located within the bulk gap. Figure 3 presents the eigenfrequency spectrum and admittance spectrum for this topological configuration. Figure 3(a) shows the calculated eigenfrequency spectrum, where states marked by red dots correspond to corner-localized states, and purple dots correspond to edge and bulk states. Three red dots are clearly visible inside the bulk gap, well separated from the edge and bulk states. Figure 3(b) displays the corresponding admittance spectrum, where the corner states manifest as prominent admittance peaks, providing clear electrical signals for experimental observation. The positions of these admittance peaks exactly match the theoretically predicted eigenfrequencies.

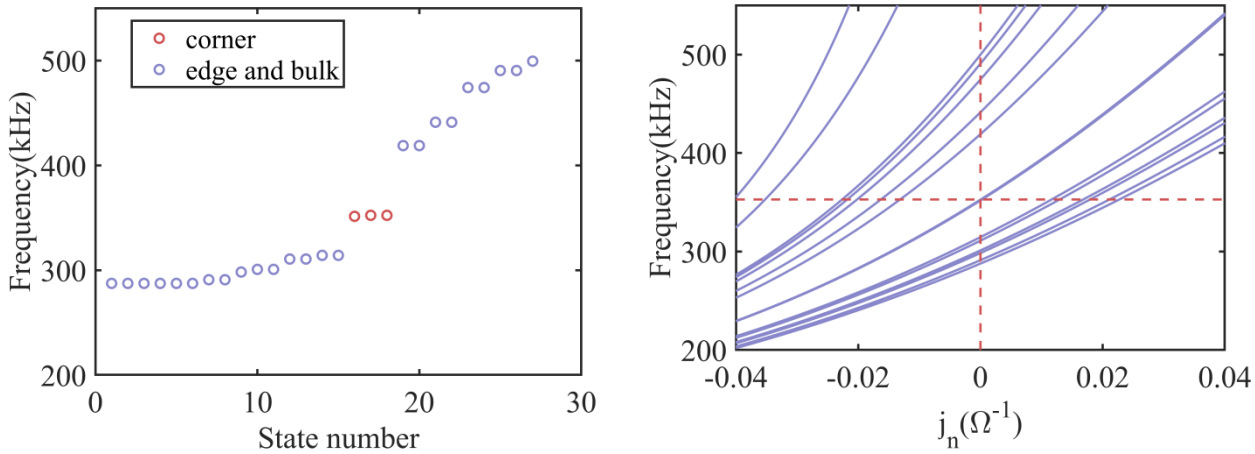

Fig. 3 (a) Calculated eigenfrequency spectrum of the topological Kagome circuit. (b) Admittance spectrum of the topological Kagome circuit. The corner states are denoted by red dots, the edge and bulk states are denoted by purple dots. They both share parameters $C_A = 2.2nF, C_B = 8nF, L = 1\mu H$.

3. Summary

In this work, we have experimentally realized a breathing kagome lattice using an electric circuit network and successfully observed higher-order topological corner states. By independently controlling the intra-cell and inter-cell coupling strengths through adjustable capacitance values, a finite-sized triangular circuit network comprising 30 nodes was constructed. When $C_A = 2.2$ nF, $C_B = 8$ nF, and $L = 1\,\mu$H, the system is placed in the topologically nontrivial regime. Through eigenfrequency spectrum calculations and admittance measurements, we directly observed three degenerate topological corner states at frequency $f =$ 352.3 kHz, located inside the bulk gap and well separated from edge and bulk states. Control experiments in the trivial configuration ($C_A = 8$ nF, $C_B = 2.2$ nF) showed no in-gap states, further validating the topological nature of the observed modes. Our results establish circuit networks as a versatile and highly tunable platform for investigating higher-order topology in frustrated lattices, offering advantages in flexibility, direct electrical readout, and reconfigurability. This work paves the way for future explorations of three-dimensional higher-order topological insulators, disorder-induced topological phases, non-Hermitian topology, and nonlinear topological effects in engineered classical systems.

References

[1] M. Z. Hasan and C. L. Kane, Colloquium : Topological insulators, Rev. Mod. Phys. 82, 3045 (2010).

[2] X.-L. Qi and S.-C. Zhang, Topological insulators and superconductors, Rev. Mod. Phys. 83, 1057 (2011).

[3] F. Schindler, A. M. Cook, M. G. Vergniory, Z. Wang, S. S. P. Parkin, B. A. Bernevig, and T. Neupert, Higher-order topological insulators, Sci. Adv. 4, eaat0346 (2018).

[4] W. A. Benalcazar, B. A. Bernevig, and T. L. Hughes, Electric multipole moments, topological multipole moment pumping, and chiral hinge states in crystalline insulators, Phys. Rev. B 96, 245115 (2017).

[5] S. Mittal, E. A. Goldschmidt, and M. Hafezi, A topological source of quantum light, Nature 561, 502 (2018).

[6] B.-Y. Xie, G.-X. Su, H.-F. Wang, H. Su, X.-P. Shen, P. Zhan, M.-H. Lu, Z.-L. Wang, and Y.-F. Chen, Visualization of Higher-Order Topological Insulating Phases in Two-Dimensional Dielectric Photonic Crystals, Phys. Rev. Lett. 122, 233903 (2019).

[7] T. Neupert, L. Santos, C. Chamon, and C. Mudry, Fractional Quantum Hall States at Zero Magnetic Field, Phys. Rev. Lett. 106, 236804 (2011).

[8] I. Syozi, Statistics of Kagome Lattice, Prog. Theor. Phys. 6, 306 (1951).

[9] M. Ezawa, Higher-Order Topological Insulators and Semimetals on the Breathing Kagome and Pyrochlore Lattices, Phys. Rev. Lett. 120, 026801 (2018).

[10] T. Hirano, H. Katsura, and Y. Hatsugai, Topological classification of gapped spin chains: Quantized Berry phase as a local order parameter, Phys. Rev. B 77, 094431 (2008).

[11] A. El Hassan, F. K. Kunst, A. Moritz, G. Andler, E. J. Bergholtz, and M. Bourennane, Corner states of light in photonic waveguides, Nat. Photonics 13, 697 (2019).

[12] X. Zhang, Z.-K. Lin, H.-X. Wang, Z. Xiong, Y. Tian, M.-H. Lu, Y.-F. Chen, and J.-H. Jiang, Symmetry-protected hierarchy of anomalous multipole topological band gaps in nonsymmorphic metacrystals, Nat. Commun. 11, 65 (2020).

[13] H. Li, T. Yamaguchi, S. Matsumoto, H. Hoshikawa, T. Kumagai, N. L. Okamoto, and T. Ichitsubo, Circumventing huge volume strain in alloy anodes of lithium batteries, Nat. Commun. 11, 1584 (2020).

[14] J. Ningyuan, C. Owens, A. Sommer, D. Schuster, and J. Simon, Time- and Site-Resolved Dynamics in a Topological Circuit, Phys. Rev. X 5, 021031 (2015).

[15] C. H. Lee, S. Imhof, C. Berger, F. Bayer, J. Brehm, L. W. Molenkamp, T. Kiessling, and R. Thomale, Topolectrical Circuits, Commun. Phys. 1, 39 (2018).

[16] S. Imhof et al., Topolectrical-circuit realization of topological corner modes, Nat. Phys. 14, 925 (2018).

[17] T. Hofmann et al., Reciprocal skin effect and its realization in a topolectrical circuit, Phys. Rev. Res. 2, 023265 (2020).